Role of the Triplet State in Retinal Photoisomerization As Studied by Laser-Induced Optoacoustic Spectroscopy†

Alessandro Feis,‡ Bas Wegewijs, Wolfgang Gärtner, and Silvia E. Braslavsky*

Max-Planck-Institut für Strahlenchemie, Postfach 10 13 65, D-45413 Mülheim an der Ruhr, Germany

Received: March 10, 1997; In Final Form: July 8, 1997⊗

Laser-induced optoacoustic spectroscopy (LIOAS) was applied to the study of 13-*cis* (13RT), 11-*cis* (11RT), and all-*trans* (trRT)-retinal photoisomerization in various *n*-alkanes. From the analysis of the LIOAS data in aerated and N_2-saturated solutions of the three isomers, it is concluded that their triplet states undergo different relaxation pathways. Whereas trRT and 11RT produce long-lived triplet states that are quenched by oxygen, yielding $O_2(^1\Delta_g)$ with high efficiency, the 13RT triplet rapidly releases its excess energy by isomerization to the trRT isomer. Direct measurement of the near-IR emission from $O_2(^1\Delta_g)$ supports these conclusions. The quantum yield for $O_2(^1\Delta_g)$ production is 0.61 ± 0.05 for trRT, 0.27 ± 0.05 for 11RT (in each case similar to the respective yield of triplet formation, as detected by LIOAS), and <0.15 for the 13RT isomer (*i.e.*, much smaller than its triplet yield). With this combination of techniques and the use of literature data, it was possible to elucidate the role of the triplet state in the photoisomerization reaction, which turned out to be different for each retinal isomer: the trRT triplet is nonreactive and loses all its excess energy by intersystem crossing to the ground state, the 11RT triplet isomerizes to the trRT triplet, and the 13RT triplet isomerizes to the trRT ground state. Furthermore, the LIOAS data for 13RT appear to be solvent dependent in the range from *n*-pentane to *n*-hexadecane, which might be interpreted in terms of a structural volume change for the *cis* → *trans* (13RT → trRT) photoisomerization. Depending on the interpretation of the data, a contraction with a value between 33 and 130 mL/mol was calculated. However, the validity of this analysis was difficult to establish, and alternative explanations of the solvent dependence such as a variation of the isomerization quantum yield could not be ruled out, due to the intrinsic, relatively large error of the quantum yield determination.

Introduction

Retinals (vitamin-A aldehydes) have attracted a broad interest owing to their peculiar photoisomerization reactions and to their biological relevance, since retinals are the chromophores of the visual pigments and of the halobacterial purple membrane protein bacteriorhodopsin.[1,2] Although the photophysics and photochemistry of several retinal isomers have been studied with respect to the photoisomerization pathways and mechanisms,[3] the photoproduct distribution,[4] and, more recently, the spectral properties of transients,[5] there is still no definite information on the dynamics of the various excited-state isomerization pathways. The largest collection of data relates to the all-*trans*-retinal (trRT) isomer. Several studies have shown that the photoisomerization of trRT proceeds through the singlet state, with a relatively low efficiency.[6−8] The photoisomerization of trRT leads to different mixtures of isomers at photoequilibrium, depending on the solvent, but the primary photoproduct is the 13-*cis*-retinal (13RT) isomer in all solvents. The opposite photoisomerization process, 13RT → trRT, is less well characterized. The efficiency of this process is higher, and both singlet and triplet pathways seem to be involved.[9]

This paper presents the results of the application of laser-induced optoacoustic spectroscopy (LIOAS) to the study of trRT, 13RT, and 11-*cis*-retinal (11RT) photoisomerization. There are several ways in which photoisomerization is reflected in the LIOAS signals. The first one is through energy release or storage due to the different heat contents of the isomers. Moreover, photoisomerization influences the dynamics of energy relaxation from the excited states, thus favoring some relaxation pathways rather than others, and this is also reflected in the LIOAS signals. A third contribution might come from structural volume changes taking place in the sample as a consequence of photoisomerization.[10] As already stated several times in the literature, thermal volume changes ΔV_{th} and structural volume changes ΔV_r add up to give the LIOAS signal amplitude H_S^n (eq 1):[10−17]

$$H_S^n = k(\Delta V_{th} + \Delta V_r) \quad (1)$$

where k contains instrumental parameters and thermoelastic parameters of the solution. In this and following equations, H_S^n represents the laser fluence-normalized LIOAS amplitude. The first term is proportional to the fraction α_S of the laser energy E_λ promptly released as heat and to the ratio of the thermoelastic parameters of the solution $\beta/c_p\rho$, where β is the cubic expansion coefficient, c_p the heat capacity at constant pressure, and ρ the mass density. The relative contribution of ΔV_{th} and ΔV_r to the LIOAS signal can be determined by varying the $c_p\rho/\beta$ ratio. The constant k is eliminated by normalizing the signal from the sample, H_S, using the signal of a calorimetric reference, H_R, for which $\Delta V_r = 0$ and $\alpha = 1$. Thus, eq 2 results:

$$H_S^n/H_R^n = \alpha_S + (\Delta V_r/E_\lambda)(c_p\rho/\beta) \quad (2)$$

$(c_p\rho/\beta)$ can be continuously varied with temperature in aqueous solutions.[10,11] For investigations of organic compounds

† Abbreviations: 2OHBP, 2-hydroxybenzophenone; LIOAS, laser-induced optoacoustic spectroscopy; 11RT, 11-*cis*-retinal; 13RT, 13-*cis*-retinal; trRT, all-*trans*-retinal; TRPD, time-resolved phosphorescence detection.

* To whom correspondence should be addressed.

‡ Present address: Dipartimento di Chimica, Università di Firenze, Via G. Capponi 9, I-50121 Firenze, Italy.

⊗ Abstract published in *Advance ACS Abstracts,* September 1, 1997.

S1089-5647(97)00879-1 CCC: $14.00 © 1997 American Chemical Society

that do not dissolve in water, it must be taken into account that for organic solvents the temperature dependence of $(c_p\rho/\beta)$ on T is very weak. Thus, it has been proposed that ΔV_r can be determined by measuring the signals of the sample and the reference in a series of homologous solvents, *e.g.*, *n*-alkanes,[12,13,15,16] with the assumptions that (i) the differential solvation between reactants and products is not remarkably different in this series and (ii) energy relaxation processes other than heat release do not depend on the solvent. Picosecond optical calorimetic measurements[15] and LIOAS measurements[16] of intramolecular electron transfer in donor−bridge−acceptor molecules dissolved in series of *n*-alkanes have yielded values of enthalpy changes in agreement with values obtained by other methods and volume changes that could be in part satisfactorily analyzed by using the continuum model for electrostriction. However, it is not completely clear whether assumption (i) is valid in the case of photoisomerizations and thus whether the approach for the separation of both contributions to the pressure signal is applicable.

Since all retinal isomers are reported to have a relatively high triplet yield ($\Phi_T = 0.4-0.7$ for trRT,[8,18] 0.5 for 11RT,[19] and 0.39 for 13RT[19]), assumption (ii) needed verification. For this purpose, we measured the quantum yield of photosensitized O_2-($^1\Delta_g$) production from aerated solutions of the retinal isomers in different alkanes. We also looked for a correlation between $O_2(^1\Delta_g)$ production and LIOAS amplitude changes under aerobic and anaerobic conditions.

Finally, an attempt was made to obtain photoisomerization quantum yields for 13RT as a function of alkane solvent, in view of the assumption that the isomerization efficiency might decrease with increasing solvent viscosity.

Experimental Section

The isomers trRT, 13RT, and 11RT were separated by preparative HPLC with >98% purity (as checked by analytical HPLC) after irradiation of a solution of trRT (Sigma) in 2-propanol (5 mM) with a 250 W tungsten halogen lamp until photoequilibrium was reached (as tested by the absorption spectrum and analytical HPLC). The isomer mixture was then separated on a silica column (Kromasil 100-Sil, 5 μm) with 2.5% diethyl ether/*n*-hexane as mobile phase. The *n*-alkane solvents were highly purified by distillation, column chromatography, preparative GC, or zone refining. Their purity was confirmed by analytical GC. 2-Hydroxybenzophenone (2OHBP) was obtained from Merck and recrystallized from ethanol.

LIOAS measurements were performed as already described.[10,16] Laser excitation was performed with the third harmonic of a Spectron SL800 Q-switched Nd:YAG laser (355 nm wavelength, 8 ns pulse length, 2 Hz repetition rate). The laser beam was attenuated with a variable glass filter and shaped with a 0.8 × 8 mm rectangular slit. The beam was not focused, so that the active volume was far from optical saturation (1:30 absorbed photon/molecules for a typical concentration and 10 μJ/pulse). The beam energy was measured by pyroelectric energy meters (Laser Precision RJP 735 or 765 heads, RJ 7620 or Rm 6600 meters). The sample was held in quartz cuvettes for absorption spectrometry with 1 cm optical path, saturated with O_2, and thermostated to 22 °C. The piezoelectric ceramic detector was clamped to the cuvette side. The detector output was amplified and fed to a digitizing oscilloscope (Tektronix 584A or 620A or LeCroy 9310). The signal acquisition was controlled by a DEC 3100 VAX station. The sample (2 mL volume, $A_{355} = 0.15-0.3$) was stirred during the measurement in order to avoid photoproduct accumulation in the active volume. The sample was changed after 100 shots with 5 μJ mean energy. Under these conditions, less than 2% photoisomerization (for 13RT) was calculated to take place in the bulk volume. We checked the photoproduct distribution by analytical HPLC and could only detect trRT formation from 13RT, while the amount of 13RT formed from trRT was undetectable. As calorimetric reference compound we used the well-tested 2OHBP; for comparison another well-known reference compound ferrocene was also used.[11] The LIOAS signals of these two references had the same magnitude within 0.5%.

The absorption spectra were measured with a Shimadzu UV-2102PC spectrophotometer. The molar absorption coefficients for the determination of the sample concentration (used for the photoisomerization quantum yield determination) were $\epsilon = 47\,400\ M^{-1}\ cm^{-1}$ for trRT and $\epsilon = 38\,800\ M^{-1}\ cm^{-1}$ for 13RT at 365 nm in *n*-hexane.[7] The absorption coefficient at 355 nm was calculated relative to these values. We checked that the absorption coefficient at the maximum did not appreciably vary in the alkane series. In fact, only a small red shift with the increasing chain length was observed. The spectra for the determination of the photoisomerization quantum yield Φ_{PI} of 13RT were fitted (with Microcal Origin software) by the sum of the absorption spectra of each pure isomer, trRT and 13RT, in the range from 300 to 450 nm. The fit parameters were related to the [trRT] and [13RT], and these were inserted into the following equation[7]

$$\Psi = (1+ E/2 + E^2/12)\ln([13RT]_0/[13RT]) + [(3 + E)/6](\epsilon'_{13RT} - \epsilon'_{trRT})[trRT]d + (1/24)(\epsilon'_{13RT} - \epsilon'_{trRT})^2 d^2(2\,[13RT]_0[trRT] - [trRT]^2) = \Phi_{PI}\,(d\epsilon'_{13RT}/V)N \quad (3)$$

where $E = \epsilon'_{trRT}d[13RT]_0$, $\epsilon' = 2.3\epsilon_{355}$, d is the optical path length, $[13RT]_0$ is the initial concentration, V is the solution volume, and N is the photon quantity in einsteins. Ψ is a corrected 13RT concentration, which takes into account absorption changes progressively taking place upon irradiation. The samples ($V = 3$ mL) for the determination of Φ_{PI} were irradiated under the same experimental conditions as for LIOAS and had similar concentrations.

Time-resolved phosphorescence from $O_2(^1\Delta_g)$ (TRPD) was measured at $\lambda > 1000$ nm as described,[20] using a North Coast N_2-cooled Ge detector upon irradiating *n*-hexane or *n*-hexadecane solutions of retinal and reference (see Results) with the same laser as for LIOAS with 30−110 μJ/pulse. The signal amplitude was obtained by extrapolation of the single-exponential decay signal to zero time. The fluorescence quantum yield of 13RT in *n*-hexadecane at $\lambda_{exc} = 355$ nm was determined by comparing the area under the emission curve to that of a standard solution of quinine sulfate in 0.1 N sulfuric acid.[21] The corrected fluorescence emission spectra were measured with a Fluorolog spectrofluorimeter.

Results

Figure 1 shows a typical laser-fluence dependence of the LIOAS signal amplitude. The LIOAS signal amplitude was measured for the sample solution and for a calorimetric reference solution under identical experimental conditions (see inset in Figure 1). The calorimetric reference was in most cases 2OHBP which is known to release all the absorbed energy as prompt heat and to have $\Delta V_r = 0$.[22,23] In some cases ferrocene was used as calorimetric reference, which gave identical signals as 2OHBP. The signal amplitude H was measured as the difference between the first maximum and the first minimum of the signal. Such signal analysis is suitable for the case of aerated

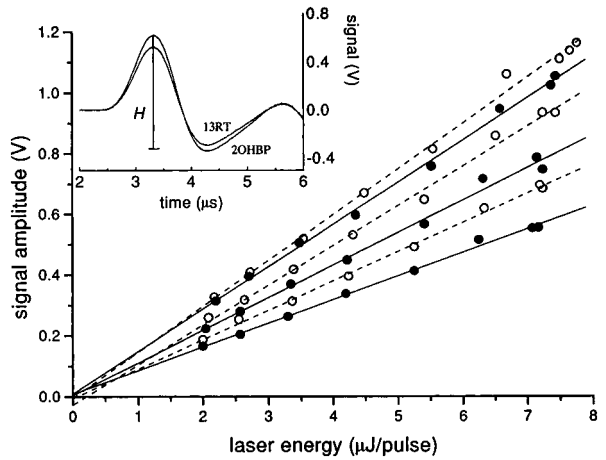

Figure 1. Fluence-dependent LIOAS amplitude from (●) 13RT and (○) 2OHBP *n*-hexadecane solutions of increasing absorption (A_{355} = 0.18, 0.26, 0.34). The amplitudes are linearly interpolated. Inset: Time-resolved LIOAS signal from 13RT in *n*-hexadecane, compared to that of the reference compound 2OHBP. The signal is the average of 25 shots with 7.2 μJ/pulse.

as well as N_2-saturated retinal solutions, since the time dependence was found to be the same for both the retinal sample and the reference. This can be explained as follows: any triplet state formed has a very short lifetime (τ_T < 20 ns) due to effective quenching by energy transfer to O_2, while the $O_2(^1\Delta_g)$ state thus formed has a very long lifetime (>30 μs) as compared to the experimental LIOAS time window. Hence, there is no transient process occurring on the detection time scale, and the heat is either released promptly or stored for a longer time. In case of measurements with N_2-saturated solutions, the triplet state can be very long-lived (up to 10 μs for trRT), which is also too long to be detected by our LIOAS system. Thus, the signal evaluation could be performed in the straightforward way mentioned above, and deconvolution methods such as those used in other systems[16] did not yield clear evidence for any transient species, except for occasional observations of the triplet decay in case of insufficient N_2 saturation (residual oxygen quenching).

In order to detect small amplitude differences in the sample and reference signals, averaging was performed at three levels: (i) Each point in Figure 1 is the average of 25 single-shot measurements. This allowed for a good signal-to-noise ratio in alkane solutions. (ii) The dependence of H on the incident laser fluence was measured for several fluence values in a range from 2 to 10 μJ/pulse, checking for linearity. The data were interpolated with a least-squares fit. (iii) The fluence dependence was measured for three samples (and references) with different absorbances, as shown in Figure 1. The slopes were plotted *vs* A and linearly interpolated to give the final LIOAS fluence-normalized amplitudes H^n for sample and reference.

Figure 2 shows the solvent dependence of the ratio H_S^n/H_R^n (the ratio of the sample and reference fluence-normalized LIOAS amplitudes) for 13RT and trRT in a series of homologous linear alkanes, *i.e.*, *n*-pentane, *n*-hexane, *n*-heptane, *n*-decane, *n*-dodecane, and *n*-hexadecane. The error bars refer to the averaging step (iii).

The data points were plotted *vs* the thermoelastic parameters ratio $c_p\rho/\beta$ for each alkane.[16] For 13RT, H_S^n/H_R^n appears to depend on the solvent. It is between 1 and 1.1 in pentane, hexane, and heptane, and it smoothly decreases to 0.93 in dodecane and to 0.92 in hexadecane.

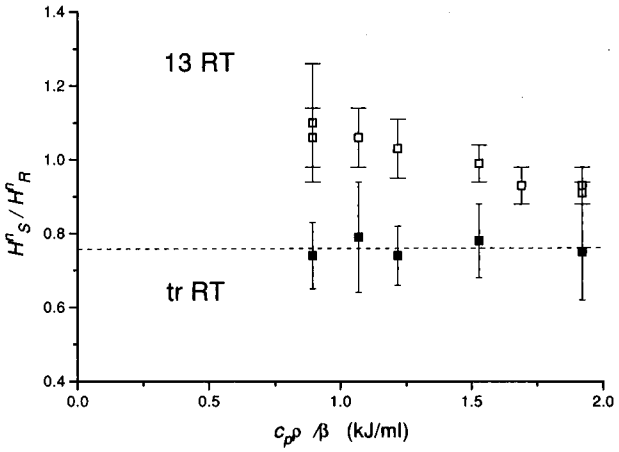

Figure 2. Solvent-dependent ratio H_S^n/H_R^n for (□) 13RT and (■) trRT in (from left to right) *n*-pentane, *n*-hexane, *n*-heptane, *n*-decane, *n*-dodecane, and *n*-hexadecane. trRT data points are linearly interpolated with a least-squares fit.

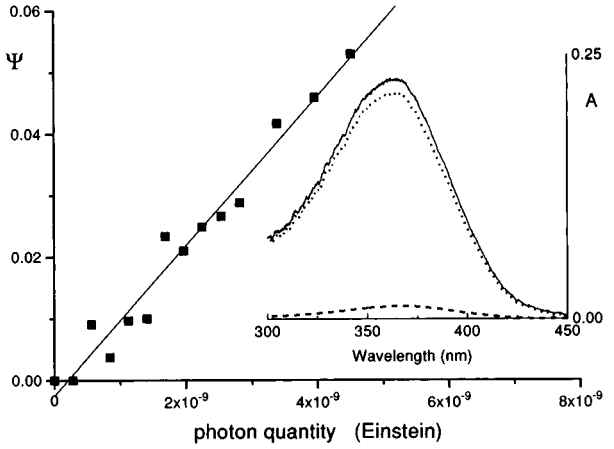

Figure 3. Photoisomerization quantum yield determination for 13RT in *n*-hexane (A_{355} = 0.22). Ψ is a corrected trRT concentration (see text). The quantum yield is the slope of the linear plot obtained from a least-squares data fitting. Inset: Absorption spectrum of the solution after irradiation with 4.5 × 10^{-9} einstein at 355 nm. A fit with the sum of the spectra of the two pure isomers is superimposed on the spectrum, and the fitting curve overlaps the measured spectrum. The spectra of the two pure isomers are also shown (···, 13RT; - - -, trRT).

In the case of trRT, there is no apparent solvent dependence and H_S^n/H_R^n is much lower than 1 for all solvents. If the trRT data points are linearly fitted, an intercept $\alpha_S = 0.76 \pm 0.05$ is obtained (eq 2).

We also measured (data not shown) the solvent dependence of the LIOAS amplitude for 11-*cis*-retinal alkane solutions. There is no evidence either for a solvent dependence of the signal for this retinal isomer within the accuracy of the measurements, and $\alpha_S = 0.93 \pm 0.05$.

Figure 3 shows a plot of Ψ *vs* photon quantity (see Experimental Section) for an *n*-hexane solution of 13RT. Similar plots were used for the determination of the photoisomerization quantum yields Φ_{PI} of 13RT in *n*-pentane, *n*-hexane, *n*-heptane, *n*-decane, and *n*-hexadecane (Table 1). We concluded that only trRT was formed from 13RT since (i) we followed the photoconversion process only up to 5% trRT formation, (ii) we checked the photoproduct distribution in 13RT samples after LIOAS (*i.e.*, after irradiation conditions very similar to those for the quantum yield determination) by means of HPLC and only found trRT, and (iii) fitting the spectra with the spectrum of 9-*cis*-retinal, besides those of trRT and 13RT, did not improve the fit. As an example of the fitting procedure,

TABLE 1: Quantum Yield of Photoisomerization Φ_{PI} for 13RT Aerated *n*-Alkane Solutions[a]

	Φ_{PI}[b]
pentane	0.48 ± 0.13 [2]
hexane	0.46 ± 0.05 [2]
heptane	0.30 ± 0.05 [1]
decane	0.42 ± 0.06 [2]
hexadecane	0.46 ± 0.05 [1]
average value	0.43 ± 0.10 [8]
hexane[7]	0.4
3-methylpentane[30]	0.21

[a] The error limits are standard deviations from the least-squares fitting in every single determination or from the average value for multiple measurements, whatever is larger. [b] Number of measurements given in brackets.

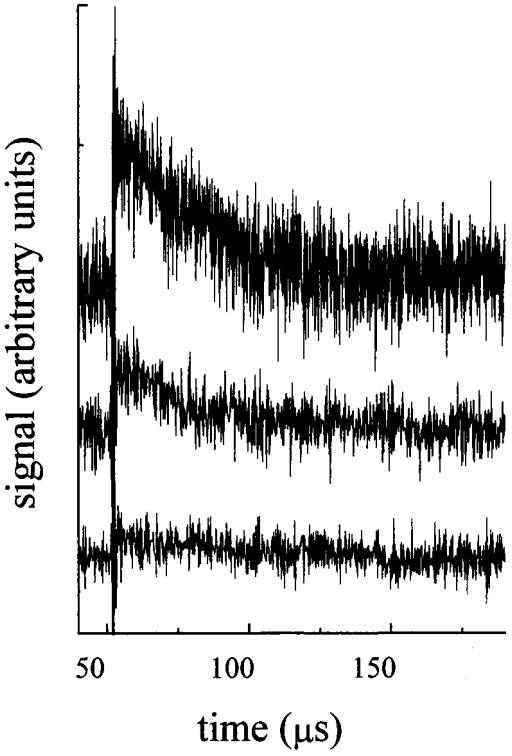

Figure 4. Time-resolved emission of $O_2(^1\Delta_g)$ from aerated solutions of (from bottom to top) 13RT ($A_{355} = 0.29$), 11RT ($A_{355} = 0.22$), and trRT ($A_{355} = 0.20$) in *n*-hexane. $\lambda_{exc} = 355$ nm, 115 μJ/pulse.

the inset in Figure 3 shows the absorption spectrum corresponding to the point with the highest Ψ in the plot, together with the two fit components, *i.e.*, the spectra of pure trRT and of pure 13RT.

Φ_{PI} is derived from the slope of the least-squares fit of the plot in Figure 3. There seems to be no significant trend in the Φ_{PI} values in the *n*-alkane series, although the error can be seen to be relatively large. A mean value $\Phi_{PI} = 0.43 \pm 0.10$ was found from eight determinations in the five selected solvents.

Figure 4 shows the decay profiles of $O_2(^1\Delta_g)$ emission determined by TRPD from solutions of trRT ($A_{355} = 0.20$), 11RT ($A_{355} = 0.22$), and 13RT ($A_{355} = 0.29$) in *n*-hexane. The amplitude was corrected in order to take into account the small absorption difference between the samples. Energy transfer to O_2 is much more efficient for trRT than for 13RT and 11RT. The quantum yield for $O_2(^1\Delta_g)$ production, Φ_Δ, was measured by comparing the single-exponential emission extrapolated at time = 0 to that of a solution of tetraphenylporphycene ($\Phi_\Delta = 0.36$)[24] and of pyrene ($\Phi_\Delta = 0.83$)[25] in *n*-hexane. The absorbance difference between sample and reference was

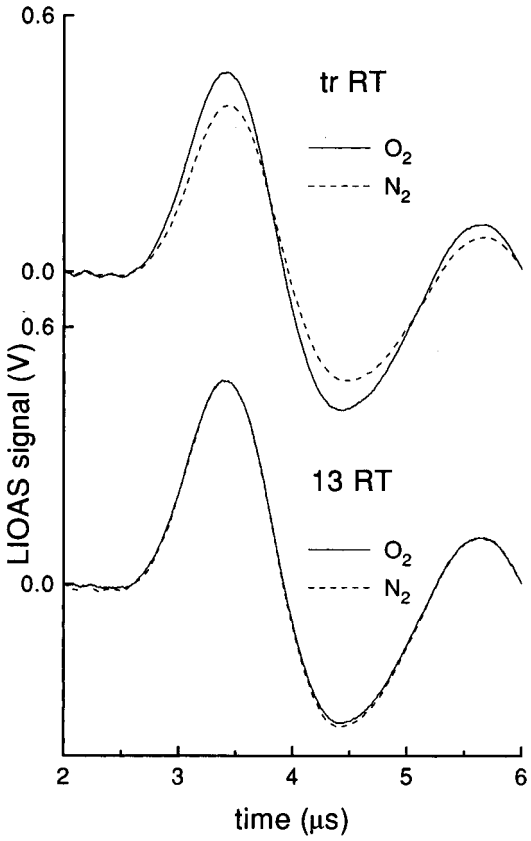

Figure 5. LIOAS signals from O_2-saturated and N_2-saturated solutions of trRT ($A_{355} = 0.36$) and 13RT ($A_{355} = 0.26$) in *n*-hexane. The signals are the average of 50 shots with 5 μJ/pulse.

corrected for by using the Lambert−Beer law. The $O_2(^1\Delta_g)$ lifetime was 30 μs, in agreement with the literature value for this solvent.[26]

For trRT, $\Phi_\Delta = 0.61 \pm 0.05$ was determined from six measurements at three energy values, while for 11RT a value of $\Phi_\Delta = 0.27 \pm 0.05$ was obtained. For 13RT, a quantitative evaluation was more difficult because of the lower signal and the higher Φ_{PI} value, which leads to the formation of the more efficient trRT after a few laser shots, and to some extent even within each laser shot. The measured yield can thus be considered as an upper limit, and it was estimated as $\Phi_\Delta < 0.10$ in *n*-hexane. A similar limit was determined for 13RT in *n*-hexadecane, *i.e.*, $\Phi_\Delta < 0.15$.

In order to consider the generation of $O_2(^1\Delta_g)$, the effect of O_2 on the LIOAS signals was analyzed. Figure 5 shows LIOAS signals from *n*-hexane solutions of 13RT and trRT with either N_2 or O_2 bubbled through the solution for 20 min before the measurement. There is a clear reduction of the LIOAS amplitude for trRT (13%) and for 11RT (13−15%, not shown) upon N_2 saturation, while the LIOAS signal for 13RT shows a slight increase (<1.5% in *n*-hexane and in *n*-hexadecane).

In order to be sure that there was no influence of the viscosity on the relative yield of the various deactivation pathways, the fluorescence quantum yield was determined for 13RT in *n*-hexadecane, and it resulted to be lower than the sensitivity of the instrumentation ($< 10^{-3}$). Another test consisted of performing LIOAS experiments of 13RT in *n*-hexadecane at slightly elevated temperature, which resulted in a significant increase in H_S^n/H_R^n from 0.92 (at $T = 22$ °C) to 0.98 (at $T = 40$ °C), while the absorption of the sample did not change over this temperature range.

Discussion

(a) Role of the Triplet State in trRT, 11RT, and 13RT Photoprocesses. The information obtained with the LIOAS measurements described above pertains to the amount of energy that is stored in long-lived transient species, which reflects the relative efficiency of the various heat release processes. In general, internal conversion and fast photoisomerization to a retinal ground-state isomer are processes that convert the initial excitation energy completely into heat, thus contributing to the prompt LIOAS signal. Energy storage can only be expected if species are produced that are longer lived than the pressure integration time (*ca.* 800 ns), such as a stable isomer, a long-lived triplet state, or $O_2(^1\Delta_g)$ produced by oxygen quenching of that triplet state.

Combining the LIOAS results with the $O_2(^1\Delta_g)$ quantum yield data and comparing them with literature data on triplet and photoisomerization quantum yields allows us to draw some clear conclusions concerning the fate of the triplet state for the three RT isomers in alkane solvents.

(i) trRT. The best characterized photoisomerization process of all retinal isomers is that of trRT. It has been shown that the photoisomerization pathway goes exclusively through the singlet state,[6] and relevant quantum yields were reported to be $\Phi_{PI} = 0.06-0.2$,[7] $\Phi_T = 0.43-0.7$,[8,18,19] and $\Phi_\Delta = 0.66$.[18]

The relative LIOAS amplitude H_S^n/H_R^n is lower than 1 in all solvents for trRT, and the intercept of the plot is 0.76 ± 0.05 (Figure 2). Since these measurements were performed in the presence of oxygen, the energy-storing pathway can be attributed to triplet energy transfer to O_2. A calculation affords the value of α_S, by using simple energy balance considerations,[11,27] when the fluorescence quantum yield is negligible and the O_2 concentration is high enough to quench all triplets (which is the case for the measurements shown in Figure 2). Thus, eq 4 results:

$$\alpha_S E_\lambda = E_\lambda - \Phi_\Delta E_\Delta - \Phi_{PI} \Delta E_{PI} \qquad (4)$$

In eq 4, $E_\Delta = 94.1$ kJ/mol is the energy content of $O_2(^1\Delta_g)$[28] and ΔE_{PI} is the energy difference between the photoisomers. However, the latter contribution can be neglected, especially in case of the trRT photoisomerization, in view of the low values of both Φ_{PI} and ΔE_{PI} (see section b.(i) of the Discussion). Using our value $\Phi_\Delta = 0.61$ for trRT, which agrees well with $\Phi_\Delta = 0.66$ obtained by flash photolysis in cyclohexane,[18] a value of $\alpha_S = 0.83$ results from eq 4. Indeed, this is similar to the intercept of the plot in Figure 2 (0.76 ± 0.05).

Furthermore, the observation that the LIOAS signal in the presence of oxygen is higher than under nitrogen conditions (Figure 5) can be explained by the extra heat release process taking place within the experimental time window, which is caused by the triplet quenching yielding the lower-energy $O_2(^1\Delta_g)$ species. From the LIOAS amplitude under N_2-saturated conditions ($\alpha_S = 0.66$) and the assumption that $\Phi_\Delta = \Phi_T$, we calculate $E_T = 154$ kJ/mol (using $\alpha_S E_\lambda = E_\lambda - \Phi_T E_T$), which is in accord with the literature value $E_T = 150-159$ kJ/mol.[29] This agreement nicely supports the validity of our measurements.

In all, our results are in good agreement with most literature data and support the view that upon photoexcitation a triplet state is formed in high quantum yield (>0.61 according to our data), which is long-lived in the absence of oxygen but relatively short-lived in the presence of oxygen due to efficient $O_2(^1\Delta_g)$ production. Eventually, the trRT triplet relaxes to the ground state of the trRT isomer and does not produce any of the *cis*-isomers.

(ii) 11RT. For 11RT, a photoisomerization quantum yield in the range of 0.12−0.25 has been reported in the literature,[7,8,30] in combination with an efficiency of 1 ± 0.2 for isomerization from the triplet state.[31] Thus, in contrast to trRT, the 11RT triplet seems to play a key role in the photoisomerization process.

From our results it can be concluded that a relatively long-lived triplet state is formed, which is almost fully quenched in the presence of oxygen. Since the energy-storing species in the LIOAS experiments is $O_2(^1\Delta_g)$, we can calculate from our value of $\alpha_S = 0.93$ (using eq 4) that $\Phi_\Delta = 0.25$. Indeed, this is very close to $\Phi_\Delta = 0.27$ directly determined by TRPD.

Assuming that Φ_T has a value similar to that of $\Phi_\Delta = 0.25$ (owing to the efficiency of the oxygen-quenching process), it is interesting to note that this value coincides with the value for the total quantum yield of photoisomerization ($\Phi_{PI} = 0.24$, $\lambda_{exc} = 360$ nm) determined by Waddell et al.[30] This is in line with the conclusion that quantitative isomerization from the 11RT triplet state to trRT takes place and that only very little isomerization from the singlet state occurs.

According to Mukai and co-workers, transient Raman[32] and time-resolved absorption spectra[33] clearly show that the 11RT triplet relaxes within 100 ps into the long-lived trRT triplet state. Such a pathway would explain the fact that the isomerization efficiency is close to unity, since all of the trRT triplet formed relaxes exclusively to the trRT ground state (see above). However, our data do not rule out the possibility of an isomerization pathway directly from the 11RT triplet to the trRT ground state. The only extra information we have is that the reduction in LIOAS signal in the absence of oxygen (owing to the higher energy level of the long-lived triplet state as compared to $O_2(^1\Delta_g)$) has the same value (13−15%) as in the case of trRT, which might be taken as an indication that 11RT relaxes to the same triplet state as trRT. In addition, most evidence in the literature is also in favor of this latter mechanism. For instance, quenching (up to 99%) of the triplet state formed by 11RT by a nitroxyl radical does not change the isomerization quantum yield,[34] which shows that it is the trRT triplet state that is quenched and not the 11RT triplet. Similarly, the quantum chain process proposed by Ganapathy and Liu[35] to account for the strongly concentration-dependent photoisomerization quantum yield of 11RT can only be explained by assuming that isomerization takes place in the triplet state, followed by energy transfer from the long-lived trRT triplet state.

Concerning the total quantum yield of photoisomerization, it is still possible that there is some small contribution to Φ_{PI} from 11RT singlet isomerization taking into account the error limits of Φ_{PI} and Φ_T (± 0.05). This pathway would be similar to that occurring in the trRT isomer.

We note in passing that our Φ_T values of 0.25 and 0.27 (as determined by LIOAS and TRPD respectively) do not agree with the literature value of $\Phi_T = 0.5$.[19] Nevertheless, we prefer to use these 0.25/0.27 values for the 11RT triplet quantum yield under our experimental conditions.

(iii) 13RT. The LIOAS amplitudes of 13RT are not constant in the range of alkane solvents studied (Figure 2). Some interpretations for this observation can be found in section (b) of the Discussion. In any case, the LIOAS amplitudes for 13RT approach unity and are clearly higher than those for trRT and for 11RT. This means that hardly any energy is stored and that no long-lived triplet state is formed. On the other hand, the triplet quantum yield of 13RT has been determined to be 0.39,[19] and the photoisomerization quantum yield amounts to 0.4−0.48 (see Table 1, compare with $\Phi_{PI} = 0.21$ in 3-methylpentane[30] and $\Phi_{PI} = 0.4$ in *n*-hexane[7]).

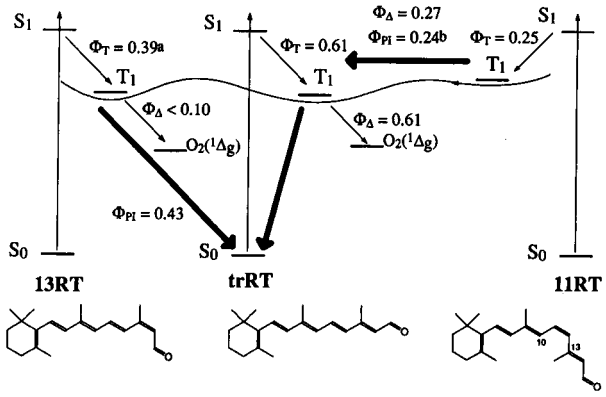

Figure 6. Schematical representation of the main pathways of triplet formation and decay for 13RT, trRT, and 11RT in *n*-alkanes, as based on LIOAS experiments, singlet oxygen measurements, and literature data ([a]ref 19; [b]ref 29). The energy levels of the various states are not drawn to scale; it can be expected that the ground and triplet states of 13RT are only slightly higher in energy than those of trRT, whereas the states of 11RT are at significantly higher energy.[43] Note that the Φ_{PI} values refer to the *total* quantum yield of photoisomerization, but that the singlet pathways of 13RT and 11RT contribute only a few percent to Φ_{PI}. The broad arrows correspond to pathways having an efficiency of virtually unity (in the absence of oxygen).

Thus, combining these three observations, it appears that all of the 13RT triplet states formed isomerize directly to ground state trRT. Only such a pathway could explain the fact that the triplet state is relatively short-lived and that its decay contributes to the *prompt* heat release signal measured within the LIOAS time-window of *ca*. 800 ns. Moreover, there is hardly any difference in LIOAS signal with or without oxygen, which implies that the triplet is quenched more quickly by the isomerization reaction than by energy transfer to oxygen. Interestingly, careful inspection of Figure 5 reveals that *if* there is a slight difference in signal for 13RT, then it is a very small *decrease* of the signal in the presence of oxygen, in contrast to the situation for trRT and 11RT (see above). This could be taken to signify that there still is a small amount of $O_2(^1\Delta_g)$ production in competition with the isomerization, storing a minute fraction of the excitation energy into $O_2(^1\Delta_g)$. Unfortunately, our Φ_Δ measurements gave no clear results, other than an upper limit of $\Phi_\Delta < 0.15$, which we attribute mostly to trRT formed during the measurements.

Mukai and co-workers found[32,33] that 13RT is the only *cis*-retinal isomer that appears to have a stationary triplet state that is spectroscopically different from that of trRT, which indeed could point to a special role of the 13RT triplet in this case. Nevertheless, they also concluded that the 13RT triplet still seems to transform mainly into the trRT triplet state, analogous to 11RT. Our LIOAS data, however, clearly indicate that such a 13RT → trRT triplet isomerization cannot be an important pathway, as this would produce the long-lived trRT triplet state, which would store a significant part of the excitation energy.

According to our results, it can be envisaged that the 13RT triplet goes to ground-state trRT through a perpendicular (phantom) state, such as in the case of stilbene photoisomerization.[36] In addition, a direct isomerization pathway through the 13RT singlet state cannot be excluded, which might contribute a few percent to the total Φ_{PI}.

To summarize this part of the discussion, our results and interpretations are presented schematically in Figure 6, where the quantum yields of the various photophysical pathways are indicated for the three retinal isomers studied. To rationalize the different behavior of 11RT and 13RT, it should be noted that 11RT is a sterically hindered isomer (because of the interaction between the 13-methyl group and the 10-hydrogen), whereas 13RT does not have such hindrance. Consequently, there is an extra driving force for 11RT to isomerize to trRT, especially on the rather shallow triplet potential energy surface, resulting in a subnanosecond isomerization process. The triplet state of 13RT is relatively stable with respect to direct isomerization, which is substantiated by the fact that its spectrum can be observed on a nanosecond time scale.[32,33] This longer lifetime opens up the possibility for 13RT to relax from its triplet state to the trRT ground state. Interestingly, the relaxation of both 13RT and trRT can be assumed to take place via the same phantom state, explaining why they should have the same *cis*/*trans* branching ratio (*i.e.* virtually all going to the *trans* ground state).

(b) Photoisomerization Volume Changes. *(i) Analysis of the LIOAS Data.* As described in the Introduction, the LIOAS technique not only detects heat-induced volume changes of the solvent but also any possible structural volume changes of the solute and solvent molecules. Therefore, LIOAS experiments should always be carried out in such a way that both contributions can be separated, to avoid errors in interpreting the magnitudes of the signals.

For trRT and 11RT we found no indication for a structural volume change, since the amplitudes remained constant over the alkane range studied. In the case of 13RT, however, a clear decrease in signal with increasing $c_p\rho/\beta$ can be seen in Figure 2.

According to eq 2, the slope of the plot H_S^n/H_R^n *vs* $c_p\rho/\beta$ is related to the photoisomerization structural volume changes, while the intercept is the energy that is promptly released as heat from the sample, α_S. A linear fit of the 13RT data points yields $\Delta V_r = -55 \pm 5$ mL/mol $= \Delta V_{PI}\Phi_{PI}$, *i.e.*, the product of the molecular photoisomerization volume change, ΔV_{PI}, times the photoisomerization quantum yield Φ_{PI}. Thus, $\Delta V_{PI} = (-127 \pm 30)$ mL/mol using the mean value $\Phi_{PI} = 0.43$ from our determination (Table 1). On the other hand, the intercept obtained from this fit is about 1.2, which makes the accuracy of the fit dubious, since the intercept is predicted to be >1 only if the energy difference between the photoisomers ΔE_{PI} is negative and considerably large ($\alpha_S = 1 - \Phi_{PI}\ \Delta E_{PI}/E_\lambda$). However, only a very small (−0.9 kJ/mol) energy difference between ground state trRT and 13RT was calculated,[37] compared to the excitation energy $E_\lambda = 336.9$ kJ/mol. Therefore, we attribute the large α_S value to the large error in the *n*-pentane measurements. We also note that using an *n*-alkane solvent series as a way of separating the two contributions to the pressure in the LIOAS experiment might result in a variable solvation enthalpy along the series, introducing a serious error.

Alternatively, we can calculate the value of $\Delta V_{PI}\Phi_{PI}$ from the data in the longer alkanes, *i.e.*, *n*-dodecane and *n*-hexadecane, assuming $\alpha_S = 1$ due to the low value of $\Phi_{PI}\ \Delta E_{PI}/E_\lambda$. Then $\Delta V_r = -14.0 \pm 0.5$ mL/mol is obtained, which corresponds to $\Delta V_{PI} = -33 \pm 8$ mL/mol.

This contraction following 13RT → trRT photoisomerization should correspond to an expansion for the trRT photoisomerization, which mainly produces 13RT in *n*-alkanes. However, the lack of the observation of a volume increase for trRT could be due to the small Φ_{PI} (0.06−0.2).[7] In fact, an expansion of 33 mL/mol in the trRT → 13RT process, *i.e.*, the same value with opposite sign of that for the 13RT → trRT photoisomerization, should give rise to an observed volume change $\Phi_{PI}\Delta V_{PI}$ of only 2−7 mL/mol, which seems too low to be detected.

(ii) Possible Origin of the Volume Change. The overall photoisomerization process we observe on the LIOAS time scale is from ground state 13RT to ground state trRT. The intrinsic

molecular volume change due to the changes in bond lengths and angles is possibly very small. More sizeable volume changes are expected to occur as a consequence of the rearrangement of the solvent around the isomerized solute.[10] A model that has been applied to correlate volume changes with changes in the electrical properties of the solute is the dielectric continuum model. In this model, solvent electrostriction is correlated with the solvent dielectric constant, the solute cavity radius r, and the change in the electrical dipole moment, $\Delta\mu$, due to the photoisomerization reaction.[15−17] An estimate of the retinal cavity yields $r^3 = 96$ Å^3.[38] With this value and the calculated change in dipole moment from 13RT to trRT in *n*-hexane solutions, 0.4 D,[37] a calculation using the Drude−Nernst formula yields a volume change due to solvent electrostriction < 1 mL/mol. On the other hand, contractions much larger (*ca.* −100 mL/mol) than those predicted by electrostriction theory have been observed in other processes in organic solvents, *e.g.*, during the ionization of CO_2 in glass-forming alkanes.[39,40]

(iii) Alternative Explanations. In order to establish the occurrence of a volume change, we checked the experimental causes potentially biasing the measured value. We stress that ΔV_{PI} is obtained from a measurement of small amplitude differences between the sample and the calorimetric reference. Negative contributions other than ΔV_{PI} to the LIOAS amplitude may stem from radiative emission or from energy storage in long-lived species such as triplet states or $O_2(^1\Delta_g)$ produced by energy transfer from the triplet. We therefore determined to what extent these processes occur for 13RT in different alkanes.

Fluorescence emission from retinals is known to have a very low quantum yield in *n*-hexane ($\Phi_f < 10^{-5}$).[41] From our emission measurement for 13RT in *n*-hexadecane, it can be ruled out that this relaxation process appreciable takes place even in the more viscous *n*-alkanes.

Furthermore, the rate of photoisomerization might decrease with increasing alkane chain length, due to an increase in solvent viscosity. This effect would lead to lower LIOAS amplitudes, since oxygen quenching would be competing with photoisomerization, resulting in a small amount of $O_2(^1\Delta_g)$ production in the more viscous alkanes such as *n*-dodecane and *n*-hexadecane. As a consequence, the value of Φ_Δ should be higher in the more viscous alkanes. Although there is no clear solvent dependence for the energy transfer to O_2, as judged from the similarity in the values of Φ_Δ in *n*-hexane (<0.10) and *n*-hexadecane (<0.15) solutions, it should be pointed out that these are only rough upper limits, and especially the true value for *n*-hexane is expected to lie close to zero in view of the LIOAS results. Therefore, no conclusion can be drawn from the Φ_Δ data.

The result of the LIOAS measurement of 13RT in *n*-hexadecane at $T = 40$ °C (where the amplitude approaches 1) might be taken as support for a viscosity-dependent photoisomerization quantum yield, as increasing the temperature might be expected to increase the rate of photoisomerization, yielding the "normal" efficiency of unity that is found in the less viscous alkanes. An argument against this interpretation is that no clear decrease of Φ_{PI} can be seen in Table 1, although these values contain relatively large error limits.

In conclusion, this alternative explanation involving a nonconstant photoisomerization rate for 13RT could be partly responsible for the trend observed in the LIOAS data in Figure 2.

Conclusions

The application of time-resolved optoacoustic spectroscopy to the study of the photoisomerization of retinals shows that the excited states of trRT, 11RT, and 13RT have different patterns of heat release pathways and store different amounts of energy after laser excitation. In combination with singlet oxygen emission data and photoisomerization quantum yields, it is possible to estimate the relative importance of the various decay pathways taking place, as shown in Figure 6.

Interestingly, the triplet state appears to have a different role in each of the three isomers studied: in trRT it is nonreactive and simply decays to the trRT ground state, in 11RT isomerization takes place on the triplet potential energy surface probably yielding the trRT triplet, and in 13RT isomerization occurs from the triplet state directly to the trRT ground state, thereby providing a relatively fast quenching mechanism of the triplet state.

These mechanisms reflect the influence of steric factors on the photophysical behavior of the retinal isomers. This is especially important for the 11RT chromophore, since the steric hindrance caused by the interaction of the 13-methyl group with the H at C-10 already facilitates a fast isomerization in the triplet state in solution. It has been suggested that the steric factor is the driving force for the optimization of the photoisomerization in the rhodopsins. The protein matrix thus acts stabilizing a highly hindered ground state conformation of 11RT already torsioned in the isomerization direction, resulting in a very fast isomerization reaction (few femtoseconds) in the singlet state that competes with radiation and radiationless deactivation.[42]

Furthermore, an attempt was made to determine the volume changes concomitant with isomerization. Only for 13RT a possible effect was seen in the solvent dependence of the LIOAS signals, leading to an estimate of ΔV_{PI} of −33 to −130 mL/mol. However, an alternative explanation in terms of viscosity-dependent photoisomerization rates seems to be equally valid, which would diminish or even nullify the presumed volume change effect.

Acknowledgment. We thank G. Koç-Weier, S. Pörting, and A. Keil-Block for the technical assistance, Dr. C. Scharnagl (München) for the MO calculations, and Professor K. Schaffner for his support. A.F. and B.W. received EU fellowships (Human Capital and Mobility Program Grant No. ERBCHBGCT930313).

References and Notes

(1) Hargrave, P. A.; McDowell, J. H. *Int. Rev. Cytol.* **1992**, *137B*, 49−97.
(2) Mathies, R. A.; Lin, S. W.; Ames, J. B.; Pollard, W. T. *Annu. Rev. Biophys. Biophys. Chem.* **1991**, *20*, 491−518.
(3) Becker, R. S. *Photochem. Photobiol.* **1988**, *48*, 369−399.
(4) Ganapathy, S.; Liu, R. S. H. *Photochem. Photobiol.* **1992**, *56*, 959−964.
(5) Tahara, T.; Toleutaev, B. N.; Hamaguchi, H. *J. Chem. Phys.* **1994**, *100*, 786−796.
(6) Yuzawa, T.; Hamaguchi, H. *J. Mol. Struct.* **1995**, 489−495.
(7) Kropf, A.; Hubbard, R. *Photochem. Photobiol.* **1970**, *12*, 249−260.
(8) Rosenfeld, T. A.; Alchalel, A.; Ottolenghi, M. *J. Phys. Chem.* **1974**, *78*, 336−341.
(9) Raubach, R. A.; Guzzo, A. V. *J. Phys. Chem.* **1973**, *77*, 889−92.
(10) Churio, M. S.; Angermund, K. P.; Braslavsky, S. E. *J. Phys. Chem.* **1994**, *98*, 1776−1782.
(11) Braslavsky, S. E.; Heibel, G. E. *Chem. Rev.* **1992**, *92*, 1381−1410.
(12) Ma, J.; Bhaskar Dutt, G.; Waldeck, D. H.; Zimmt, M. B. *J. Am. Chem. Soc.* **1994**, *116*, 10619−10629.
(13) Hung, R. R.; Grabowski, J. J. *J. Am. Chem. Soc.* **1992**, *114*, 351−353.
(14) Herman, M. S.; Goodman, J. L. *J. Am. Chem. Soc.* **1989**, *111*, 1849−1854.
(15) Morais, J.; Zimmt, M. B. *J. Phys. Chem.* **1995**, *99*, 8863−8871.
(16) Wegewijs, B.; Verhoeven, J. W.; Braslavsky, S. E. *J. Phys. Chem.* **1996**, *100*, 8890−8894.
(17) Morais, J.; Ma, J.; Zimmt, M. B. *J. Phys. Chem.* **1991**, *95*, 3885−3888.

(18) Chattopadhyay, S. K.; Kumar, C. V.; Das, P. K. *J. Photochem.* **1984**, *24*, 1−9.
(19) Bensasson, R.; Land, E. J.; Truscott, T. G. *Photochem. Photobiol.* **1975**, *21*, 419−421.
(20) Martínez, G.; Bertolotti, S. G.; Zimerman, O. E.; Mártire, D. O.; Braslavsky, S. E.; García, N. A. *J. Photochem. Photobiol. B* **1993**, *17*, 247−255.
(21) Eaton, D. F. *Pure Appl. Chem.* **1988**, *60*, 1107−1114.
(22) Van Haver, P.; Viaene, L.; Van der Auweraer, M.; De Schryver, F. C. *J. Photochem. Photobiol. A* **1992**, *63*, 265−277.
(23) Burkey, T. J.; Majewski, M.; Griller, D. *J. Am. Chem. Soc.* **1986**, *108*, 2218−2221.
(24) Nonell, S.; Aramendía, P. F.; Heihoff, K.; Negri, R. M.; Braslavsky, S. E. *J. Phys. Chem.* **1990**, *94*, 5879−5883.
(25) D. M. Shold, *J. Photochem.* **1978**, *8*, 39−48.
(26) Salokhiddinov, K. I.; Byteva, I. M.; Gurinovich, G. P. *J. Appl. Spectrosc.* **1981**, *34*, 561−566.
(27) Losi, A.; Bedotti, R.; Viappiani, C. *J. Phys. Chem.* **1995**, *99*, 16162−16167.
(28) Gilmore, F. R. *J. Quant. Spectrosc. Radiat. Transfer* **1965**, *5*, 369−389.
(29) Rosenfeld, T.; Kalisky, O.; Ottolenghi, M. *J. Phys. Chem.* **1977**, *81*, 1496−1498.
(30) Waddell, W. H.; Crouch, R.; Nakanishi, K.; Turro, N. J. *J. Am. Chem. Soc.* **1976**, *98*, 4189−4192.
(31) Jensen, N. H.; Wilbrandt, R.; Bensasson, R. V. *J. Am. Chem. Soc.* **1989**, 111, 7877−7888.
(32) Hamaguchi, H.; Okamoto, H.; Tasumi, M.; Mukai, Y.; Koyama, Y. *Chem. Phys. Lett.* **1984**, *107*, 355−359.
(33) Mukai, Y.; Koyama, Y.; Hirata, Y.; Mataga, N. *J. Phys. Chem.* **1988**, 92, 4649−4653.
(34) Kuzmin, V. A.; Kliger, D. S.; Hammond, G. S. *Photochem. Photobiol.* **1980**, *31*, 607−609.
(35) Ganapathy, S.; Liu, R. S. H. *J. Am. Chem. Soc.* **1992**, *114*, 3459−3464.
(36) Görner, H.; Kuhn, H. J. *Adv. Photochem.* **1995**, *19*, 1−117.
(37) Scharnagl, C. Personal communication.
(38) Myers, A. B.; Birge, R. R. *J. Am. Chem. Soc.* **1981**, *103*, 1881−1885.
(39) Ninomiya, S.; Itoh, K.; Nishikawa, M.; Holroyd, R. *J. Phys. Chem.* **1993**, *97*, 9488−9492.
(40) Schwarz, H. A. *J. Phys. Chem.* **1993**, *97*, 12954−12958.
(41) Takemura, T.; Das, P. K.; Hug, G.; Becker, R. S. *J. Am. Chem. Soc.* **1978**, *100*, 2626−2630.
(42) Kochendoerfer, G. G.; Mathies, R. A. *Isr. J. Chem.* **1995**, *35*, 211−226.
(43) Sperling, W.; Carl, P.; Rafferty, C. N.; Dencher, N. A. *Biophys. Struct. Mech.* **1977**, *3*, 79−94.